

# 1 **Strain-level diversity impacts cheese rind microbiome assembly and** 2 **function**

3

4

5 Running title: Strain-level diversity in cheese rind microbiomes

6

7 Brittany A. Niccum<sup>1</sup>, Erik K. Kastman<sup>1</sup>, Nicole Kfoury<sup>2,3</sup>, Albert Robbat Jr.<sup>2,3</sup>, Benjamin E.  
8 Wolfe<sup>1,3</sup>

9

10 <sup>1</sup>Tufts University, Department of Biology, Medford, MA, USA

11 <sup>2</sup>Tufts University, Department of Chemistry, Medford, MA, USA

12 <sup>3</sup>Tufts University Sensory and Science Center, Medford, MA, USA

13

14 \*Correspondence: [benjamin.wolfe@tufts.edu](mailto:benjamin.wolfe@tufts.edu)

15

16

17

18 **ABSTRACT** Taxa that are consistently found across microbial communities are often  
19 considered members of a core microbiome. One common assumption is that  
20 taxonomically identical core microbiomes will have similar dynamics and functions  
21 across communities. However, strain-level genomic and phenotypic variation of core  
22 taxa could lead to differences in how core microbiomes assemble and function. Using  
23 cheese rinds, we tested whether taxonomically identical core microbiomes isolated from  
24 distinct locations have similar assembly dynamics and functional outputs. We first  
25 isolated the same three bacterial species (*Staphylococcus equorum*, *Brevibacterium*  
26 *auranticum*, and *Brachybacterium alimentarium*) from nine cheeses produced in  
27 different regions of the United States and Europe. Comparative genomics identified  
28 distinct phylogenetic clusters and significant variation in genome content across the  
29 nine core microbiomes. When we assembled each core microbiome with initially  
30 identical compositions, community structure diverged over time resulting in communities

31 with different dominant taxa. The core microbiomes had variable responses to abiotic  
32 (high salt) and biotic (the fungus *Penicillium*) perturbations, with some communities  
33 showing no response and others substantially shifting in composition. Functional  
34 differences were also observed across the nine core communities, with considerable  
35 variation in pigment production (light yellow to orange) and composition of volatile  
36 organic compound profiles emitted from the rinds (nutty to sulfury). Our work  
37 demonstrates that core microbiomes isolated from independent communities may not  
38 function in the same manner due to strain-level variation of core taxa. Strain-level  
39 diversity across core cheese rind microbiomes may contribute to variability in the  
40 aesthetics and quality of surface-ripened cheeses.

41

42

## 43 **INTRODUCTION**

44 Metagenomic surveys of microbial communities often describe the existence of  
45 core microbiomes. Although many definitions currently exist (1), core microbiomes are  
46 generally considered to be the set of microbial taxa that are commonly found across all  
47 (or many) sampled microbial communities. Many microbiomes, from plant roots to  
48 wastewater treatment plants, contain a set of core taxa that are common, highly  
49 abundant, and functionally significant (1–4). These core microbiomes can range from  
50 just a few species to tens or hundreds of species. For example, most human skin  
51 microbiomes are dominated by very similar *Corynebacterium*, *Propionibacterium*, and  
52 *Staphylococcus* species (3, 5, 6).

53           One largely untested assumption is that taxonomically identical core  
54 microbiomes will have similar community assembly patterns and functions. More  
55 specifically, when comparing 16S rRNA gene sequencing surveys, samples that have  
56 very similar compositions of 16S sequences are often assumed to have similar  
57 functional potentials. This assumption underlies the development of taxonomy-based  
58 microbiome diagnostics and tools used to predict function from taxonomic sequences  
59 (7, 8). But independent evolution or coevolution of microbial species within communities  
60 may generate previously underappreciated functional diversity across core  
61 microbiomes. It is widely accepted that microbial genomes are highly variable within  
62 species due to rapid rates of evolution and potential for lateral gene transfer (9–11).  
63 Moreover, we know from decades of work in microbial ecology, physiology, and  
64 genomics that there is considerable within species trait variation in microbes (12–14).  
65 For example, a set of 11 strains of *Brevundimonas alba* isolated from the same  
66 freshwater habitat had identical 16S rRNA sequences, but highly divergent carbon  
67 utilization profiles and growth rates (15). This intraspecific trait diversity could be  
68 ecologically significant, but the impact of strain-level diversity on core microbiome  
69 assembly and function is poorly understood (16).

70           Cheese rinds provide an ideal opportunity to test whether taxonomically identical  
71 core microbiomes have similar assembly dynamics and functions and more generally  
72 the causes and consequences of core microbiome diversification. Rinds form on the  
73 surfaces of cheeses aged in an aerobic environment and are composed of bacteria,  
74 yeasts, and filamentous fungi (17–19). Our previous work used amplicon and shotgun  
75 metagenomics to describe the bacterial and fungal diversity of 137 cheese rinds from

76 the United States and Europe (17). Three bacterial genera - *Staphylococcus*,  
77 *Brevibacterium*, and *Brachybacterium* - were the most frequently detected across  
78 cheese rinds and can be considered a core microbiome. Through variation in abiotic  
79 and biotic selection pressures applied during cheese production and aging, including  
80 abiotic (salinity, pH, resource availability) and biotic (presence of bacterial and fungal  
81 neighbors), core cheese microbiomes have the potential to evolve new genotypes and  
82 phenotypes with divergent functions.

83 Here we characterize core microbiome members across cheese rind  
84 communities and determine the consequences of core microbiome diversification for  
85 community assembly and function. We isolated the same three species of bacteria -  
86 *Staphylococcus equorum* (hereafter *Staphylococcus*), *Brevibacterium auranticum*  
87 (hereafter *Brevibacterium*), and *Brachybacterium alimentarium* (hereafter  
88 *Brachybacterium*) - from nine different cheeses made across the United States and  
89 Europe (**Fig. 1A-B**). These nine sets of three co-isolated bacterial species are referred  
90 to as ***taxonomically identical core microbiomes*** throughout the rest of the paper  
91 (**Fig. 1C**). The three taxa represent the most common species of the three most  
92 abundant bacterial genera in cheese rinds (17, 20). *Staphylococcus*, *Brevibacterium*,  
93 and *Brachybacterium* enter the dairy environment from the raw milk used for cheese  
94 production and therefore have the potential to co-occur and adapt to abiotic and biotic  
95 conditions within local cheese production facilities (21–23). Each species has a distinct  
96 colony morphology (**Fig. 1B**) making it easy to track composition in experimental  
97 communities. We predicted that intraspecific variation of core microbiome members  
98 across cheese rind communities would cause differences in community structure over

99 time. We also predicted that strain-level diversity across core microbiomes would result  
100 in differences in community functions relevant for cheese aging, including pigmentation  
101 of the cheese rind biofilm and the production of aroma compounds.

## 102 **RESULTS**

### 103 **Variation in genome content across taxonomically identical core microbiomes**

104 To determine genomic variation across the nine taxonomically identical core  
105 microbiomes, we constructed draft genomes of each strain (**Table S1**). We used single-  
106 nucleotide polymorphisms (SNPs) in the core genes shared across all nine communities  
107 to determine phylogenomic divergence of each of the core communities (24). We then  
108 determined variation in functional gene content across the nine core communities using  
109 PGAP (25). For functional gene content analysis, we focused on accessory genes that  
110 were uniquely present in only one community as these genomic traits may help drive  
111 divergence in core microbiome functions.

112 Across the nine communities, 8,069 gene clusters were shared among all three  
113 species, making up the core metagenome of these communities. Using SNPs identified  
114 in this core metagenome with PanSeq, clear phylogenomic divergence across the nine  
115 cheese communities was apparent (**Fig. 2**). C1 was distant from the other eight core  
116 microbiomes, driven by the highly divergent *Staphylococcus* genome in this community.  
117 The eight other core microbiomes clustered into two broad phylogenomic groups: one  
118 containing C6 and C2, and the other containing the remaining six communities (**Fig. 2**).

119 The total number of unique accessory gene clusters across the nine communities  
120 was highly variable, ranging from 246 (C5) to 630 genes (C3) (**Fig. 2, Table S2**).  
121 Variability in the abundance of accessory gene clusters was most prominent in

122 *Staphylococcus* (ranging from 36-280 unique gene clusters across strains) and  
123 *Brevibacterium* (ranging from 72-213 unique gene clusters) suggesting that these taxa  
124 have the most dynamic accessory gene content in the cheese rind core metagenome.

125 Several biological processes were significantly enriched in core communities  
126 (**Table S3**). C3 had the most diverse enrichment of SEED categories, with  
127 overrepresentation of genes in potassium metabolism, carbohydrates, and DNA  
128 metabolism. Protein metabolism and phages/prophages/transposable  
129 elements/plasmids were overrepresented in C4. In C2, the accessory genome was  
130 significantly enriched with stress response genes. Carbohydrate-related genes were  
131 enriched in the C6 core microbiome. Some of these unique accessory genes could be  
132 functionally significant in the cheese rind environment. For example, *Brevibacterium* of  
133 C3 has a unique potassium transport system with high similarity to the *kdfABCF* operon  
134 (**Table S2**) that is known to play a role in salt stress in bacteria (26).

135 Collectively these genomic data demonstrate that taxonomically identical core  
136 microbiomes isolated from distinct cheeses are phylogenomically diverse and have  
137 variable genome content. Although the presence/absence of genes does not indicate  
138 actual functional potential of microbes, these comparative genomic data suggested to  
139 us that there could be divergence in how each taxa functioned within each community  
140 and how they responded to perturbations.

### 141 **Community assembly dynamics vary across taxonomically identical core** 142 **microbiomes**

143 We next determined whether strain-level differences impacted how the cheese  
144 rind communities assemble. A typical community succession in our lab model involves

145 the following steps: 1) early colonization of *Staphylococcus* that can tolerate the low pH  
146 (5.0-5.2) of the cheese curd, 2) growth of *Brachy bacterium* in middle succession, and 3)  
147 dominance by *Brevibacterium* at the end of succession (17, 27). We predicted two  
148 different potential impacts of strain-level variation on community assembly. In one  
149 scenario, distinct strains of *Staphylococcus*, *Brachy bacterium*, and *Brevibacterium*  
150 across the nine communities may vary in genome content or growth rates in isolation,  
151 but these differences may be too minor to impact the dynamics of assembly of the  
152 three-member community. In this case, we expected nearly identical community  
153 composition across the different core microbiomes as strains of each species behaved  
154 similarly. Alternatively, strain-level differences may translate into differences in  
155 interactions with other community members or rates of growth within the community  
156 succession. In this scenario, we expected to observe reproducible changes in the  
157 composition of the communities as they assembled and differences in functional  
158 outputs.

159 To determine how strain-level differences across communities impact assembly  
160 dynamics, we used *in vitro* community assembly assays to measure total colony forming  
161 units (CFU) and community composition (relative abundance of each species) (**Fig. 3A**).  
162 Communities were quantified at three and ten days after inoculating equal amounts of  
163 each of the three bacterial species on the surface of cheese curd agar. Our previous  
164 work demonstrated that this assay mimics *in situ* community dynamics (17, 27). We  
165 acknowledge that real cheese rind communities would develop over much longer time  
166 scales (weeks to months). In the context of this work, we used the community assembly

167 assay in a standardized environment to demonstrate the *potential* for divergence in  
168 community assembly.

169 At both three and ten days of community assembly, there were nearly no  
170 differences in total community abundance as measured by combined CFU of all three  
171 species (**Fig 3B**, Day 3 ANOVA  $F_{8,81} = 2.07$ ,  $P = 0.05$ ; Day 10 ANOVA  $F_{8,79} = 0.46$ ,  $P =$   
172  $0.88$ ). However, there were substantial differences in community composition across the  
173 nine core communities (Day 3 permutational multivariate analysis of variance  
174 [PERMANOVA]  $F = 4.005$ ,  $P = 0.0001$ ; Day 10 PERMANOVA  $F = 5.57$ ,  $P = 0.0001$ ).  
175 Many communities (C1, C2, C6, C7) were dominated by *Brevibacterium* at the end of  
176 succession (**Fig 3C**). Some communities had a relatively even mix of all three species  
177 (C5, C3, C8, and C9). Community C4 had a very dissimilar structure with a high  
178 abundance of *Brachybacterium* at the end of succession and a low abundance of  
179 *Brevibacterium*.

180 A simple explanation for differences in community composition across the nine  
181 core communities is that individual bacterial strains have different growth abilities alone  
182 and in the community. Those taxa and strains that grow best alone and with the  
183 community present should be the most abundant members of the community. To test  
184 this, we determined total growth of each of the 27 strains on cheese curd agar and  
185 compared growth alone after ten days to growth in the community. All *Staphylococcus*  
186 species grew well alone and had limited responses to growth in the community (**Fig.**  
187 **3D**). Two strains were slightly stimulated by growth in the community (C5 and C7) and  
188 one was slightly inhibited (C6). In contrast to the relatively even growth of the  
189 *Staphylococcus*, the *Brevibacterium* strains had variable growth alone across the nine



190 core communities. Four of the *Brevibacterium* strains grew poorly by themselves on  
191 cheese curd agar (C2, C5, C8, and C9) and were strongly stimulated by growth in the  
192 community. One *Brevibacterium* strain (C4) was inhibited by growth in the community.  
193 All *Brachybacterium* strains grew well on cheese curd by themselves and were  
194 generally inhibited when grown in the community.

195 For all three taxa, mean growth alone was a very poor predictor of mean relative  
196 abundance in the community (*Staphylococcus*  $r^2 = 0.166$ ,  $P = 0.276$ ; *Brevibacterium*  $r^2 =$   
197  $0.001$ ,  $P = 0.923$ ; *Brachybacterium*  $r^2 = 0.020$ ,  $P = 0.716$ ). A somewhat better predictor  
198 of mean relative abundance was how growth of each strain was impacted by the  
199 community (*Staphylococcus*  $r^2 = 0.672$ ,  $P < 0.01$ ; *Brevibacterium*  $r^2 = 0.013$ ,  $P = 0.773$ ;  
200 *Brachybacterium*  $r^2 = 0.319$ ,  $P = 0.113$ ). This suggests that interactions between each  
201 of the strains and their communities may contribute to differences in community  
202 composition across the nine core microbiomes. For example, the inhibition of  
203 *Brevibacterium* and lack of inhibition of *Brachybacterium* in C4 may partly explain why  
204 this community was the only one to be dominated by *Brachybacterium*.

205

## 206 **Variation in responses to abiotic and biotic perturbation across core** 207 **microbiomes**

208 Core microbiomes may experience abiotic or biotic perturbations that could alter  
209 community assembly and function. We predicted that if individual core members have  
210 evolved different responses to stress or if the communities have coevolved stress-  
211 response mechanisms, taxonomically identical core microbiomes may have divergent  
212 responses to perturbations. Two major perturbations in cheese rind core microbiomes

213 are salt and interactions with fungi (17, 20, 28). Salt concentrations are initially high on  
214 the surface of fresh cheese because salt is applied to the cheese surface or via a brine  
215 (29). The salt diffuses into the cheese and eventually equilibrates to around 3% salt in  
216 the rind environment of many cheeses. Core cheese rind microbiomes also experience  
217 interactions with fungi, ranging from yeasts (e.g. *Debaryomyces* and *Galactomyces*  
218 species) to molds (*Fusarium*, *Scopulariopsis*, and *Penicillium* species) (17, 20, 30).  
219 *Penicillium* species are widespread in cheese rinds and can strongly inhibit diverse  
220 cheese rind bacteria (17, 27, 31) potentially through the production of secondary  
221 metabolites or other mechanisms.

222 To determine how the nine core microbiomes respond to salt and fungal  
223 perturbations, we used the same community assembly assay described above with the  
224 addition of two treatments: a 6% NaCl treatment and a +*Penicillium* treatment. We used  
225 a strain of *Penicillium* that was isolated from a natural rind cheese and was previously  
226 demonstrated to inhibit cheese rind bacterial growth (17). Across isolates of all three  
227 taxa, both the 6% NaCl and +*Penicillium* treatments caused a general decrease in total  
228 growth across all nine core microbiomes with +*Penicillium* causing stronger growth  
229 inhibition (**Fig. 4A**). Core microbiomes had variable responses to the two perturbations.  
230 The *Penicillium* perturbation caused the most significant shifts in community  
231 composition with six out of nine core communities showing significant changes in  
232 community composition (**Fig. 4B-C**). In some communities, *Penicillium* caused a major  
233 increase in *Brachybacterium* relative abundance (C2 and C3). In others, *Penicillium*  
234 caused an increase in the relative abundance of *Staphylococcus* (C1, C8, and C9). The  
235 6% salt treatment caused fewer shifts in community composition with only two

236 communities (C5 and C6) responding to the higher salt environment. In both cases,  
237 *Brevibacterium* increased in relative abundance.

### 238 **Strain-level diversity of cheese rind core microbiomes drives divergent pigment** 239 **and aroma production**

240 Our experiments above demonstrate that strain-level diversity of the core cheese  
241 rind taxa drives divergence in community composition across the nine core  
242 microbiomes. Does this divergence lead to cheeses with different properties that could  
243 be perceived by consumers? Differences in community composition may not  
244 necessarily translate into differences in functional outputs. Many studies of the  
245 microbiome have suggested that communities with different compositions may have  
246 similar functions due to functional redundancy across community members (32–34).  
247 While our comparative genomic analysis above suggested potential functional  
248 differences across the cheese communities, many of the core community functions  
249 were conserved in the core genome and variation in accessory genes may have little  
250 impact on community functions. To determine whether divergence in composition of the  
251 core microbiomes also translated into differences in functional outputs, we measured  
252 two important traits of cheese rind microbiomes: rind color and volatile organic  
253 compound (VOC) production.

254 Cheese rind bacteria define how the cheese appears to customers through the  
255 production of cellular pigments such as carotenoids or the secretion of pigmented  
256 extracellular metabolites into the curd (35–39). The three bacteria in our model  
257 community produce distinct pigments (**Fig. 1B**) and shifts in their relative abundance  
258 could translate into changes in rind color. Using a colorimeter, we measured rind color

259 after 10 days. Communities had significantly different color development (ANOVA  $F_{9,39}$   
260 = 524.9,  $P < 0.0001$ ), with C3, C4, C6, C7, and C9 having significantly greater  $a^*$  values  
261 compared to the control, indicating more red pigmentation (**Fig. 5A**). All communities  
262 had significantly greater  $b^*$  values compared to the control (ANOVA  $F_{9,39} = 139.6$ ,  $P$   
263  $< 0.0001$ ), with C3 and C4 having the greatest values and appearing the most orange  
264 (**Fig. 5A**).

265 As the rind biofilm decomposes fats, proteins, and other components of the  
266 cheese substrate, a diversity of VOCs are produced that are aromatic (40–42). Using  
267 headspace sorptive extraction (HSSE) followed by gas chromatography-mass  
268 spectrometry (GC-MS) analysis (43, 44), we quantified VOCs produced by each  
269 community after 10 days of cheese rind development. Across all nine communities 248  
270 unique VOCs were detected with significant differences in the mean VOCs per  
271 community (**Fig. 5B**, ANOVA  $F_{8,35} = 28.9$ ,  $P < 0.0001$ ). The composition of VOCs across  
272 the nine cheese communities was significantly different (**Fig. 5C**, PERMANOVA  $F =$   
273 62.38,  $P < 0.001$ , **Table S4**). Using a SIMPER analysis, nine compounds contributed  
274 more than 1% to the average overall Bray-Curtis dissimilarity: benzyl methyl ketone  
275 (27% contribution; odor = floral/fruity), tetramethylpyrazine (19%; odor =  
276 nutty/musty/chocolate/coffee), 2,5-dimethylpyrazine (13%; odor =  
277 nutty/musty/chocolate/coffee), trimethylpyrazine (12%; odor =  
278 nutty/musty/chocolate/coffee), dimethyl disulfide (9%; odor = sulfurous/cabbage/onion),  
279 dimethyl trisulfide (2%; odor = sulfurous/cabbage/onion), 2,6-diethylpyrazine (2%; odor  
280 = nutty/musty/chocolate/coffee), unknown compound 520 (1%; odor = unknown), and 3-  
281 hydroxy-2-butanone (1%; odor = sweet/buttery/creamy). C5 had the most distinct VOC

282 profile of all communities with high amounts of tetramethylpyrazine, trimethylpyrazine,  
283 and 3-hydroxy-2-butanone and low amounts of the major sulfur compounds, suggesting  
284 a nuttier and more buttery aroma profile.

285

286

## 287 **DISCUSSION**

288 Using taxonomically identical three-member communities isolated from nine  
289 distinct cheeses, our work demonstrates the significance of strain-level variation for  
290 microbiome community assembly and function. Studies of plant and animal  
291 communities have demonstrated that intraspecific genetic and phenotypic diversity can  
292 impact community assembly and function (45–47). Here we demonstrate that  
293 intraspecific diversity of taxonomically identical core microbiome members can impact  
294 the relative abundance of community members as well as functional outputs of the  
295 communities. Many communities did converge on a similar composition despite having  
296 substantial variation in accessory gene content. But several communities had  
297 substantially different structures and functions even though the initial inoculum was  
298 identical. Some communities had relatively even coexistence of the three community  
299 members, while others were dominated by either *Brevibacterium* or *Brachybacterium*.  
300 The divergence was not due to stochastic community assembly across replicates as we  
301 observed highly reproducible community structures across replicate experiments.

302 The goal of this work was to determine whether taxonomically identical core  
303 microbiomes have similar community dynamics and functions. The limited number of  
304 core communities (nine) makes it difficult to pinpoint specific ecological or genetic

305 mechanisms that may be underlying the observed differences across the core  
306 communities. One simple explanation for the dominance of different taxa across the  
307 core microbiomes is differences in growth of individual strains. Our experiments  
308 comparing growth alone versus in the community demonstrates variable growth rates  
309 and interactions with the community for each of the three taxa. However, it does not  
310 fully explain community structure. For example, in C4 where *Brachybacterium*  
311 dominated, the *Brachybacterium* strain had similar levels of growth alone and  
312 interactions with community members as other communities where *Brevibacterium*  
313 dominated (e.g. C5 and C6). Future work exploring the roles of inhibitory and  
314 cooperative interactions will pinpoint specific mechanisms explaining the variable  
315 community assembly dynamics of cheese rind core microbiomes.

316         The evolutionary processes that have generated the divergent species and  
317 community-level responses of our core cheese microbiomes are currently unknown. It is  
318 possible that each core microbiome has experienced different evolutionary histories in  
319 each cheese production environment. As new batches of cheese are introduced to a  
320 cave environment, communities may be repeatedly transferred to these new cheeses.  
321 This repeated colonization of the cheese substrate could allow each of the core  
322 microbiomes to evolve collectively as a community in the individual production  
323 environments (48). Each environment may have unique abiotic selection pressures,  
324 including salt concentrations, milk composition, and temperature that could shape the  
325 evolutionary trajectories of these communities. The core microbiomes could also  
326 experience highly divergent biotic environments. For example, these core communities  
327 were isolated from cheeses with variable fungal environments, ranging from yeast to

328 filamentous fungi (17). Future work using experimental evolution to attempt to create  
329 divergent communities from an ancestral core microbiome should begin to help us  
330 understand the drivers of core microbiome diversification.

331 Our model communities represent the widespread bacterial taxa found in cheese  
332 rinds. We acknowledge that these communities have several constraints that may  
333 impact translation of our results to other systems. First, our communities only had three  
334 bacterial species. While some widespread microbiomes have low species diversity (5,  
335 49), many microbiomes have much higher levels of diversity. Would taxonomically  
336 identical core microbiomes with higher taxonomic diversity also demonstrate divergence  
337 in assembly and functions? With greater potential for higher-order interactions and a  
338 higher number of potential functions with increasing species diversity, we predict that  
339 increasing diversity may lead to even more divergent communities. Our model  
340 communities also used a single strain of each species within each core microbiome. In  
341 constructing our communities, we chose to ignore potential intraspecific variation within  
342 each of the nine core communities and assumed that the isolated taxa represented the  
343 most common genomic type of the species within each of the core communities.  
344 Metagenomic sequencing studies have identified multiple co-existing strains of the  
345 same microbial species (3, 16, 56–60) and these strains may interact with each other  
346 and other community members to impact community composition. It would be  
347 fascinating to see how including intraspecific diversity within core microbiomes may  
348 impact community assembly and function.

349 In a large amplicon-sequencing study of cheese rind microbiomes, we  
350 demonstrated that taxonomically identical cheese rind communities could form in very

351 different cheese-making regions (17). This was surprising given that these cheeses  
352 have divergent sensory properties. Many of these differences could be driven by  
353 ingredients, length of aging, or other cheese processes. Our current findings suggest  
354 that the variability in the qualities of surface-ripened cheeses could also be driven by  
355 strain-level differences across the cheese communities. We acknowledge that our lab  
356 cheese rinds are not real cheeses and only represent potential patterns of cheese rind  
357 community assembly. But it is very likely that the differences observed across the nine  
358 core microbiomes would translate to actual cheese production. Previous studies of  
359 fermented food microbes have pointed out strain-level differences of individual species  
360 used in fermented foods (50–54), but studies demonstrating the functional significance  
361 of strain-level variation at the community level are rare (55). To help preserve the  
362 unique identities of cheeses made in specific regions, it may be helpful for cheese  
363 producers to identify the unique genomic and functional properties of their core  
364 microbiomes and maintain these communities.

365 More broadly, our work in these model microbiomes may have implications for  
366 both the design and management of core microbiomes in other systems. First, our work  
367 demonstrates that taxonomic profiling of microbiomes may not provide useful predictors  
368 of assembly dynamics and functions. Amplicon based approaches of sequencing  
369 microbiomes, such as using 16S rRNA gene sequencing, only capture high-level  
370 taxonomic diversity. As we have demonstrated, taxonomically similar communities can  
371 have very different dynamics. Fortunately, microbiome sequencing studies are moving  
372 toward shotgun-metagenomic approaches that could capture the strain-level diversity  
373 that we observed across our nine communities (3, 16, 56–60). Our work also suggests



374 that it might be hard to predict microbiome responses to disturbances using taxonomic  
375 profiles alone. For example, across individuals that have similar skin core microbiomes,  
376 responses to environmental stresses such as antibiotics may depend on the specific  
377 strains and genomic content of the core communities. Finally, when designing synthetic  
378 microbiomes, our work suggests that the individual ‘parts’ (strains of species) may alter  
379 desired outcomes.

380

## 381 **METHODS**

### 382 **Isolation and maintenance of core microbiome members**

383 Frozen glycerol stocks of communities initially characterized using metagenomic  
384 sequencing (Wolfe et al. 2014) were plated out on plate count agar with milk and salt  
385 (PCAMS) to culture bacteria. Colonies with morphotypes that had the appearance of  
386 one of the three target species were streaked from single colonies. *Staphylococcus*  
387 *equorum* colonies are usually fast-growing, smooth, medium-sized, flat, and either white  
388 or light golden in color. *Brevibacterium auranticum* colonies are usually slow-growing,  
389 medium-sized, and orange. *Brachybacterium alimentarium* colonies have medium  
390 growth rates, are large and flat, and are yellow-green in color. Initial identification of the  
391 isolates was done using the 16S rRNA region using primers 27f and 1492r.

### 392 **Comparative genomics**

393 The genome of each bacterial strain was sequenced, assembled, and annotated  
394 as we previously described for *Staphylococcus* species (27). Briefly, DNA was extracted  
395 using MoBio PowerSoil DNA extraction kits from pure cultures grown for one week on  
396 PCAMS. Approximately 1 µg of purified gDNA was sheared using a Covaris S220 to  
397 approximately 450 base pair lengths and was used as the input for a New England Biolabs

398 NEBNext Ultra DNA Library Prep Kit for Illumina. Libraries were spread across multiple  
399 sequencing lanes with other projects and were sequenced using 100 base-pair, paired-end  
400 reads on an Illumina HiSeq 2500. Approximately 10 million reads were sequenced for each  
401 genome. Failed reads were removed from libraries and reads were trimmed to remove low  
402 quality bases and were assembled to create draft genomes using the *de novo* assembler in  
403 CLC Genomics Workbench 8.0. Assembled genomes were annotated using RAST(61). All  
404 genome assemblies have been deposited in NCBI (accession numbers in Table S1).

405 To identify phylogenomic relationships between each of the nine core  
406 communities, we used PanSeq (24) to identify SNPs across the core genome of each of  
407 the nine genomes for each of the three species. A SNP file for each species from each  
408 community was then concatenated together to create a community SNP file. RAxML  
409 8.2.11 (with GTR GAMMA nucleotide model and 100 bootstrap replicates) was used to  
410 create a maximum likelihood phylogeny of the nine communities using the SNP file.

411 To compare the presence and absence of genes across strains and species,  
412 core and accessory genes were identified by assigning protein-coding sequences to  
413 functionally orthologous groups using the MultiParanoid method of the PanGenome  
414 Analysis Pipeline (PGAP) (25). Species-to-species orthologs were identified by pairwise  
415 strain comparison using BLAST with PGAP defaults: a minimum local coverage of 25%  
416 of the longer group and a global match of no less than 50% of the longer group, a  
417 minimum score value of 50, and a maximum E value of  $1E-8$ . Multistrain orthologs were

418 then found using MultiParanoid (80). Enrichment of SEED subsystem categories in  
419 each of the nine core communities was determined using Fisher's exact test with false-  
420 discovery rate correction.

### 421 **Community assembly assays**

422 To measure assembly of the distinct core communities, approximately 20,000  
423 CFU of each species was inoculated on the surface of 150  $\mu$ L of cheese curd agar (3%  
424 salt) distributed into replicate wells of a 96-well plate, as previously described (17, 27).  
425 Communities were incubated aerobically at 24°C in the dark, and harvested at 3 and 10  
426 days after inoculation, which represent early and late community succession (17). To  
427 determine community composition of individual replicate communities, the community  
428 was pestled in 600  $\mu$ L of 1X phosphate buffered saline, serially diluted, and plated onto  
429 PCAMS. PCAMS plates were incubated for a week before counting the abundance of  
430 each bacterial species. To measure growth alone, the same density of CFU of each  
431 taxa alone was inoculated into wells. Five technical replicates of each community were  
432 performed in each of two experimental replicates.

433 Salt (6%) and fungal (+*Penicillium*) perturbation experiments were conducted  
434 using the same community assembly assay, but with 6% salt cheese curd agar or with  
435 the addition of *Penicillium*. *Penicillium* strain #12, isolated from a natural rind cheese in  
436 Vermont, was used in these experiments. We used this strain because it was isolated  
437 from a cheese where the *Staphylococcus*, *Brachybacterium*, and *Brevibacterium* were  
438 also found and it was used in previous experiments in our lab (27, 31). The exact  
439 species identification of this mold is unknown, but it belongs to section *Fasciculata* with

440 other cheese *Penicillium* species. *Penicillium* was inoculated at an initial density of 2000  
441 CFUs. Community composition in these experiments was determined as described  
442 above except that cycloheximide was added to PCAMS plates used for bacterial  
443 community isolation to eliminate fungal growth.

#### 444 **Color and VOC analyses**

445 To measure rind color and VOC production, we constructed larger versions of  
446 each of the nine core communities on cheese curd agar poured into Petri dishes (60mm  
447 wide) to allow for a larger sampling area. To construct the rind communities, 600,000  
448 CFU of each species was inoculated across the surface of the cheese curd agar.  
449 Experimental cheeses were incubated for 10 days in the dark at 24°C before color and  
450 VOC analyses.

451 To measure differences in color of the experimental cheeses, we used a CTI  
452 A6CTI10 spectrophotometer. This handheld colorimeter uses the CIELAB color space to  
453 quantify both lightness ( $L^*$ ) and two chromatic coordinates ( $a^*$  and  $b^*$ ). Similar  
454 colorimeters have been used to quantify cheese rind color (62). Higher values of  $a^*$   
455 ( $a^{*+}$ ) indicate red colors while lower values ( $a^{*-}$ ) indicate green colors. Higher values of  
456  $b^*$  ( $b^{*+}$ ) indicate yellow while lower values ( $b^{*-}$ ) indicate blue colors. Colorimeter  
457 readings were taken by placing a 30mm Petri dish lid upside down on the middle of the  
458 surface of the rind and then placing the colorimeter on the Petri dish surface. This was  
459 done to protect the colorimeter from the sticky rind surface and to avoid cross-  
460 contamination across replicates.

461 Cheese volatiles were collected from experimental cheese rinds by headspace  
462 sorptive extraction (HSSE) using a polydimethylsiloxane (PDMS) coated magnetic stir-

463 bar. HSSE is an equilibrium-driven, enrichment technique in which 10mm long x 0.5 mm  
464 thick stir-bars, Twister<sup>TM</sup> (Gerstel), were suspended 1 cm above the sample by placing a  
465 magnet on the top side of the collection vessel cover. Five replicates of each culture  
466 were sampled for four hours. After collection, the stir-bar was removed and spiked with  
467 10 ppm ethylbenzene-d<sub>10</sub>, an internal standard obtained from RESTEK. The internal  
468 standard was used to determine the relative concentration of each compound. Organics  
469 were introduced into the gas chromatograph/mass spectrometer (GC/MS) by thermal  
470 desorption. In addition to Twister blanks, analysis of the cheese curd agar media was  
471 made to assess background interferences. Compounds present at equal or higher  
472 relative concentrations in the media compared to the samples were removed from the  
473 data.

474 Analyses were performed using an Agilent 7890A/5975C GC/MS equipped with  
475 an automated multi-purpose sampler (Gerstel). The thermal desorption unit (TDU,  
476 Gerstel) provided splitless transfer of the sample from the stir bar into a programmable  
477 temperature vaporization inlet (CIS, Gerstel). The TDU was heated from 40°C (0.70  
478 min) to 275°C (3 min) at 600°C/min under 50ml/min of helium. After 0.1 min the CIS,  
479 operating in solvent vent mode, was heated from -100°C to 275°C (5 min) at 12°C/s.  
480 The GC column (30 m x 250 µm x 0.25 µm HP5-MS, Agilent) was heated from 40°C (1  
481 min) to 280 °C at 5°C/min with 1.2 mL/min of constant helium flow. The MS was  
482 scanned from 40 to 350 *m/z*, with the EI source at 70 eV. A standard mixture of C7 to  
483 C30 n-alkanes (Sigma–Aldrich) was used to calculate the retention index (RI) of each  
484 compound in the sample.

485           The Ion Analytics spectral deconvolution software (Gerstel) was used to analyze  
486 the GC/MS data (63, 64). A target/nontarget data analysis approach was employed  
487 where previously constructed databases are used to identify target compounds in the  
488 sample based on spectra deconvolution of their ions and abundances. Once found,  
489 each compound's mass spectrum was subtracted from the peak's total ion current (TIC)  
490 signal. Each resulting peak scan was inspected to determine if residual ion signals were  
491 constant ( $\pm 20\%$ ) or approximated background noise. If constant, the software recorded  
492 the retention time, mass spectrum, 3-5 target ions and their relative abundances into the  
493 database. Finally, sample data were compared to reference compound data in the  
494 database, viz., RI and MS (positive identification), or to commercial libraries and  
495 literature (tentative identification). Once assigned, the database was annotated to  
496 include compound name, CAS#, and RI. If neither positive nor tentative identification  
497 was possible (an unknown), a numerical identifier was used to identify the compound.  
498 The database was annotated to include the same GC/MS information described above.  
499 In contrast, if peak scans differed (an unresolved peak), the software searched for 3-5  
500 invariant scans, averaged their spectra, and then subtracted the average spectrum from  
501 the TIC signal. This process was repeated until the residual signal at each scan  
502 approximated background noise. If peak signals failed to meet the user-defined criterion  
503 below, no additional information was obtained.

#### 504 **Statistical Analyses**

505           To determine differences in community composition with all core microbiome  
506 experiments, PERMANOVAs with Bray-Curtis dissimilarity were used. ANOVA on log-  
507 transformed data was used to determine significant differences between total CFU

508 across experiments. In the cases of unequal variances (the individual taxa growth in  
509 perturbations), Kruskal-Wallis tests were used. To determine relationships between  
510 relative abundance and growth of individual strains, linear regressions were used. To  
511 compare total growth alone to growth in the community, t-tests were used. Differences  
512 in  $a^*$  and  $b^*$  values in the pigmentation assay were determined using ANOVA. To  
513 determine differences in VOC composition across the nine communities,  
514 PERMANOVAs on Bray-Curtis dissimilarity of relative peak area were used. A SIMPER  
515 analysis of relative peak area of VOCs was used to identify the contributions of each  
516 VOC to Bray-Curtis dissimilarity.

517

#### 518 **REFERENCES:**

- 519 1. Shade A, Handelsman J. 2012. Beyond the Venn diagram: the hunt for a core microbiome.  
520 *Environ Microbiol* 14:4–12.
- 521 2. Lundberg DS, Lebeis SL, Paredes SH, Yourstone S, Gehring J, Malfatti S, Tremblay J,  
522 Engelbrekton A, Kunin V, del Rio TG, Edgar RC, Eickhorst T, Ley RE, Hugenholtz P,  
523 Tringe SG, Dangl JL. 2012. Defining the core *Arabidopsis thaliana* root microbiome. *Nature*  
524 488:86–90.
- 525 3. Oh J, Byrd AL, Park M, NISC Comparative Sequencing Program, Kong HH, Segre JA.  
526 2016. Temporal stability of the human skin microbiome. *Cell* 165:854–866.
- 527 4. Albertsen M, Hansen LBS, Saunders AM, Nielsen PH, Nielsen KL. 2012. A metagenome of  
528 a full-scale microbial community carrying out enhanced biological phosphorus removal.  
529 *ISME J* 6:1094–1106.
- 530 5. Oh J, Byrd AL, Deming C, Conlan S, NISC Comparative Sequencing Program, Kong HH,  
531 Segre JA. 2014. Biogeography and individuality shape function in the human skin  
532 metagenome. *Nature* 514:59–64.

- 533 6. Findley K, Oh J, Yang J, Conlan S, Deming C, Meyer JA, Schoenfeld D, Nomicos E, Park  
534 M, NIH Intramural Sequencing Center Comparative Sequencing Program, Kong HH, Segre  
535 JA. 2013. Topographic diversity of fungal and bacterial communities in human skin. *Nature*  
536 498:367–370.
- 537 7. Aßhauer KP, Wemheuer B, Daniel R, Meinicke P. 2015. Tax4Fun: predicting functional  
538 profiles from metagenomic 16S rRNA data. *Bioinformatics* 31:2882–2884.
- 539 8. Nagpal S, Haque MM, Mande SS. 2016. Vikodak--A modular framework for inferring  
540 functional potential of microbial communities from 16S metagenomic datasets. *PLoS One*  
541 11:e0148347.
- 542 9. Toft C, Andersson SGE. 2010. Evolutionary microbial genomics: insights into bacterial host  
543 adaptation. *Nat Rev Genet* 11:465–475.
- 544 10. McAdams HH, Srinivasan B, Arkin AP. 2004. The evolution of genetic regulatory systems in  
545 bacteria. *Nat Rev Genet* 5:169–178.
- 546 11. Thomas CM, Nielsen KM. 2005. Mechanisms of, and barriers to, horizontal gene transfer  
547 between bacteria. *Nat Rev Microbiol* 3:711–721.
- 548 12. Hahn MW, Jezberová J, Koll U, Saueressig-Beck T, Schmidt J. 2016. Complete ecological  
549 isolation and cryptic diversity in *Polynucleobacter* bacteria not resolved by 16S rRNA gene  
550 sequences. *ISME J* 10:1642–1655.
- 551 13. van der Woude MW, Bäumlér AJ. 2004. Phase and antigenic variation in bacteria. *Clin*  
552 *Microbiol Rev* 17:581–611, table of contents.
- 553 14. Cohan FM. 2002. What are bacterial species? *Annu Rev Microbiol* 56:457–487.
- 554 15. Jaspers E, Overmann J. 2004. Ecological significance of microdiversity: identical 16S rRNA  
555 gene sequences can be found in bacteria with highly divergent genomes and  
556 ecophysologies. *Appl Environ Microbiol* 70:4831–4839.
- 557 16. Leventhal GE, Boix C, Kuechler U, Enke TN, Sliwerska E, Holliger C, Cordero OX. 2018.  
558 Strain-level diversity drives alternative community types in millimetre-scale granular



- 559 biofilms. *Nat Microbiol* 3:1295–1303.
- 560 17. Wolfe BE, Button JE, Santarelli M, Dutton RJ. 2014. Cheese rind communities provide  
561 tractable systems for in situ and in vitro studies of microbial diversity. *Cell* 158:422–433.
- 562 18. Wolfe BE, Dutton RJ. 2015. Fermented foods as experimentally tractable microbial  
563 ecosystems. *Cell* 161:49–55.
- 564 19. Button JE, Dutton RJ. 2012. Cheese microbes. *Curr Biol* 22:R587–R589.
- 565 20. Irlinger F, Layec S, Hélinck S, Dugat-Bony E. 2015. Cheese rind microbial communities:  
566 diversity, composition and origin. *FEMS Microbiol Lett* 362:1–11.
- 567 21. Quigley L, O’Sullivan O, Beresford TP, Paul Ross R, Fitzgerald GF, Cotter PD. 2012. High-  
568 throughput sequencing detects subpopulations of bacteria not previously associated with  
569 artisanal cheeses. *Appl Environ Microbiol* AEM.00918–12.
- 570 22. Quigley L, O’Sullivan O, Stanton C, Beresford TP, Ross RP, Fitzgerald GF, Cotter PD.  
571 2013. The complex microbiota of raw milk. *FEMS Microbiol Rev* 37:664–698.
- 572 23. Verdier-Metz I, Gagne G, Bornes S, Monsallier F, Veisseire P, Delbès-Paus C, Montel M-C.  
573 2012. Cow teat skin, a potential source of diverse microbial populations for cheese  
574 production. *Appl Environ Microbiol* 78:326–333.
- 575 24. Laing C, Buchanan C, Taboada EN, Zhang Y, Kropinski A, Villegas A, Thomas JE, Gannon  
576 VPJ. 2010. Pan-genome sequence analysis using Panseq: an online tool for the rapid  
577 analysis of core and accessory genomic regions. *BMC Bioinformatics* 11:461.
- 578 25. Zhao Y, Wu J, Yang J, Sun S, Xiao J, Yu J. 2012. PGAP: pan-genomes analysis pipeline.  
579 *Bioinformatics* 28:416–418.
- 580 26. Price-Whelan A, Poon CK, Benson MA, Eidem TT, Roux CM, Boyd JM, Dunman PM,  
581 Torres VJ, Krulwich TA. 2013. Transcriptional profiling of *Staphylococcus aureus* during  
582 growth in 2 M NaCl leads to clarification of physiological roles for Kdp and Ktr K<sup>+</sup> uptake  
583 systems. *MBio* 4.
- 584 27. Kastman EK, Kamelamela N, Norville JW, Cosetta CM, Dutton RJ, Wolfe BE. 2016. Biotic

- 585 interactions shape the ecological distributions of *Staphylococcus* species. *MBio* 7:e01157–  
586 16.
- 587 28. Monnet C, Landaud S, Bonnarne P, Swennen D. 2015. Growth and adaptation of  
588 microorganisms on the cheese surface. *FEMS Microbiol Lett* 362:1–9.
- 589 29. Fox PF, Uniacke-Lowe T, McSweeney PLH, O'Mahony JA. 2015. Chemistry and  
590 Biochemistry of Cheese, p. 499–546. *In* Fox, PF, Uniacke-Lowe, T, McSweeney, PLH,  
591 O'Mahony, JA (eds.), *Dairy Chemistry and Biochemistry*. Springer International Publishing,  
592 Cham.
- 593 30. Marcellino N, Benson DR. 2013. The good, the bad, and the ugly: tales of mold-ripened  
594 cheese. *Microbiol Spectr* 1:CM-0005-2012.
- 595 31. Zhang Y, Kastman EK, Guasto JS, Wolfe BE. 2018. Fungal networks shape dynamics of  
596 bacterial dispersal and community assembly in cheese rind microbiomes. *Nat Commun*  
597 9:336.
- 598 32. Louca S, Parfrey LW, Doebeli M. 2016. Decoupling function and taxonomy in the global  
599 ocean microbiome. *Science* 353:1272–1277.
- 600 33. Vieira-Silva S, Falony G, Darzi Y, Lima-Mendez G, Garcia Yunta R, Okuda S, Vandeputte  
601 D, Valles-Colomer M, Hildebrand F, Chaffron S, Raes J. 2016. Species–function  
602 relationships shape ecological properties of the human gut microbiome. *Nature*  
603 *Microbiology* 1:16088.
- 604 34. Allison SD, Martiny JBH. 2008. Colloquium paper: resistance, resilience, and redundancy in  
605 microbial communities. *Proc Natl Acad Sci U S A* 105 Suppl 1:11512–11519.
- 606 35. Dufossé L, Mabon P, Binet A. 2001. Assessment of the coloring strength of *Brevibacterium*  
607 *linens* strains: spectrophotometry versus total carotenoid extraction/quantification. *J Dairy*  
608 *Sci* 84:354–360.
- 609 36. Leclercq-Perlat M-N, Spinnler H-E. 2010. The type of cheese curds determined the  
610 colouring capacity of *Brevibacterium* and *Arthrobacter* species. *J Dairy Res* 77:287–294.

- 611 37. Leclercq-Perlat MN, Corrieu G, Spinnler HE. 2004. The color of *Brevibacterium linens*  
612 depends on the yeast used for cheese deacidification. *J Dairy Sci* 87:1536–1544.
- 613 38. Galaup P, Sutthiwong N, Leclercq-Perlat M-N, Valla A, Caro Y, Fouillaud M, Guérard F,  
614 Dufossé L. 2015. First isolation of *Brevibacterium* sp. pigments in the rind of an industrial  
615 red-smear-ripened soft cheese. *Int J Dairy Technol* 68:144–147.
- 616 39. Kamelamela N, Zalesne M, Morimoto J, Robbat A, Wolfe BE. 2018. Indigo- and indirubin-  
617 producing strains of *Proteus* and *Psychrobacter* are associated with purple rind defect in a  
618 surface-ripened cheese. *Food Microbiol* 76:543–552.
- 619 40. McSweeney PLH. 2004. Biochemistry of cheese ripening. *Int J Dairy Technol* 57:127–144.
- 620 41. Irlinger F, Mounier J. 2009. Microbial interactions in cheese: implications for cheese quality  
621 and safety. *Curr Opin Biotechnol* 20:142–148.
- 622 42. Fox PF, Cogan TM. 2004. Factors that Affect the Quality of Cheese, p. 583–608. *In* *Cheese*  
623 *Chemistry, Physics and Microbiology*. Elsevier.
- 624 43. Baltussen E, Sandra P, David F, Cramers C. 1999. Stir bar sorptive extraction (SBSE), a  
625 novel extraction technique for aqueous samples: theory and principles. *J Microcolumn Sep*  
626 11:737–747.
- 627 44. Müller A, Faubert P, Hagen M, Zu Castell W, Polle A, Schnitzler J-P, Rosenkranz M. 2013.  
628 Volatile profiles of fungi--chemotyping of species and ecological functions. *Fungal Genet*  
629 *Biol* 54:25–33.
- 630 45. Booth RE, Grime JP. 2003. Effects of genetic impoverishment on plant community diversity.  
631 *J Ecol*.
- 632 46. Violle C, Enquist BJ, McGill BJ, Jiang L, Albert CH, Hulshof C, Jung V, Messier J. 2012.  
633 The return of the variance: intraspecific variability in community ecology. *Trends Ecol Evol*  
634 27:244–252.
- 635 47. Siefert A. 2012. Incorporating intraspecific variation in tests of trait-based community  
636 assembly. *Oecologia* 170:767–775.

- 637 48. Lawrence D, Fiegna F, Behrends V, Bundy JG, Phillimore AB, Bell T, Barraclough TG.  
638 2012. Species interactions alter evolutionary responses to a novel environment. *PLoS Biol*  
639 10:e1001330.
- 640 49. Willger SD, Grim SL, Dolben EL, Shipunova A, Hampton TH, Morrison HG, Filkins LM,  
641 O'Toole GA, Moulton LA, Ashare A, Sogin ML, Hogan DA. 2014. Characterization and  
642 quantification of the fungal microbiome in serial samples from individuals with cystic  
643 fibrosis. *Microbiome*.
- 644 50. Bartowsky EJ, Borneman AR. 2011. Genomic variations of *Oenococcus oeni* strains and  
645 the potential to impact on malolactic fermentation and aroma compounds in wine. *Appl*  
646 *Microbiol Biotechnol* 92:441–447.
- 647 51. Orlic S, Redzepovic S, Jeromel A, Herjavec S, Iacumin L. 2007. Influence of indigenous  
648 *Saccharomyces paradoxus* strains on Chardonnay wine fermentation aroma. *Int J Food Sci*  
649 *Technol* 42:95–101.
- 650 52. Cano-García L, Flores M, Belloch C. 2013. Molecular characterization and aromatic  
651 potential of *Debaryomyces hansenii* strains isolated from naturally fermented sausages.  
652 *Food Res Int* 52:42–49.
- 653 53. Spus M, Li M, Alexeeva S, Wolkers-Rooijackers JCM, Zwietering MH, Abee T, Smid EJ.  
654 2015. Strain diversity and phage resistance in complex dairy starter cultures. *J Dairy Sci*  
655 98:5173–5182.
- 656 54. Walsh AM, Crispie F, Daari K, O'Sullivan O, Martin JC, Arthur CT, Claesson MJ, Scott KP,  
657 Cotter PD. 2017. Strain-level metagenomic analysis of the fermented dairy beverage nunu  
658 highlights potential food safety risks. *Appl Environ Microbiol* 83:e01144-17.
- 659 55. Erkus O, de Jager VCL, Spus M, van Alen-Boerrigter IJ, van Rijswijck IMH, Hazelwood L,  
660 Janssen PWM, van Hijum SAFT, Kleerebezem M, Smid EJ. 2013. Multifactorial diversity  
661 sustains microbial community stability. *ISME J* 7:2126–2136.
- 662 56. Li SS, Zhu A, Benes V, Costea PI, Hercog R, Hildebrand F, Huerta-Cepas J, Nieuwdorp M,

- 663 Salojärvi J, Voigt AY, Zeller G, Sunagawa S, de Vos WM, Bork P. 2016. Durable  
664 coexistence of donor and recipient strains after fecal microbiota transplantation. *Science*  
665 352:586–589.
- 666 57. Scholz M, Ward DV, Pasolli E, Tolio T, Zolfo M, Asnicar F, Truong DT, Tett A, Morrow AL,  
667 Segata N. 2016. Strain-level microbial epidemiology and population genomics from shotgun  
668 metagenomics. *Nat Methods* 13:435–438.
- 669 58. Asnicar F, Manara S, Zolfo M, Truong DT, Scholz M, Armanini F, Ferretti P, Gorfer V,  
670 Pedrotti A, Tett A, Segata N. 2017. Studying vertical microbiome transmission from mothers  
671 to infants by strain-level metagenomic profiling. *mSystems* 2:e00164-16.
- 672 59. Ercolini D. 2017. Exciting strain-level resolution studies of the food microbiome. *Microb*  
673 *Biotechnol* 10:54–56.
- 674 60. Turaev D, Rattei T. 2016. High definition for systems biology of microbial communities:  
675 metagenomics gets genome-centric and strain-resolved. *Curr Opin Biotechnol* 39:174–181.
- 676 61. Aziz RK, Bartels D, Best AA, DeJongh M, Disz T, Edwards RA, Formsma K, Gerdes S,  
677 Glass EM, Kubal M, Meyer F, Olsen GJ, Olson R, Osterman AL, Overbeek RA, McNeil LK,  
678 Paarmann D, Paczian T, Parrello B, Pusch GD, Reich C, Stevens R, Vassieva O, Vonstein  
679 V, Wilke A, Zagnitko O. 2008. The RAST Server: rapid annotations using subsystems  
680 technology. *BMC Genomics* 9:75.
- 681 62. Dufossé L, Galaup P, Carlet E, Flamin C, Valla A. 2005. Spectrocolorimetry in the CIE  
682 L\*a\*b\* color space as useful tool for monitoring the ripening process and the quality of PDO  
683 red-smear soft cheeses. *Food Res Int* 38:919–924.
- 684 63. Kfoury N, Baydakov E, Gankin Y, Robbat A. 2018. Differentiation of key biomarkers in tea  
685 infusions using a target/nontarget gas chromatography/mass spectrometry workflow. *Food*  
686 *Research International* 113:414-423.
- 687 64. Robbat A Jr, Kfoury N, Baydakov E, Gankin Y. 2017. Optimizing targeted/untargeted  
688 metabolomics by automating gas chromatography/mass spectrometry workflows. *J*

689 Chromatogr A 1505:96–105.

690

## 691 **ACKNOWLEDGEMENTS**

692 Esther Miller, Grace Cox, Elizabeth Landis, Freddy Lee, and Megan Biango-Daniels  
693 provided very helpful feedback on earlier drafts of this manuscript. This work was  
694 supported by NSF grant 1715553 to B.E.W.

695

## 696 **AUTHOR CONTRIBUTIONS**

697 B.E.W. isolated the bacterial strains from the nine original cheeses. B.A.N. designed,  
698 conducted, and analyzed all *in vitro* cheese experiments. N.K. and A.R. designed and  
699 performed the VOC data collection and analysis. E.K.K. and B.E.W. performed  
700 bioinformatic analyses. B.A.N. and B.E.W. performed statistical analyses on the  
701 community assembly and functional assays. B.A.N., E.E.K., N.K., A.R., and B.E.W.  
702 wrote the manuscript.

703

## 704 **COMPETING INTERESTS STATEMENT**

705 The authors declare no competing interests with one exception; A.R. developed the Ion  
706 Analytics software that is sold by Gerstel.

707

708

709

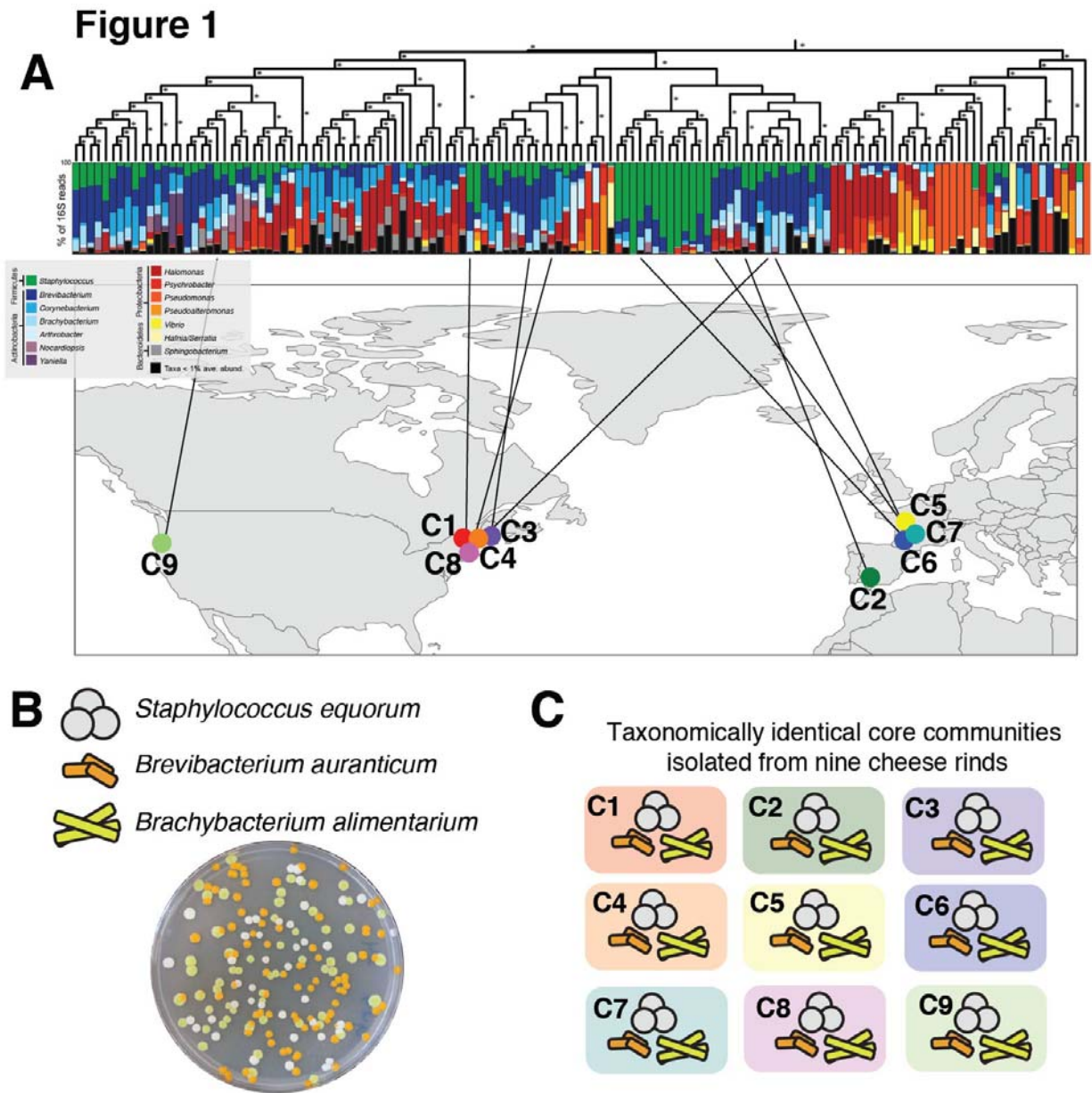
710

711

712

713

714 **FIGURES and FIGURE LEGENDS:**



715

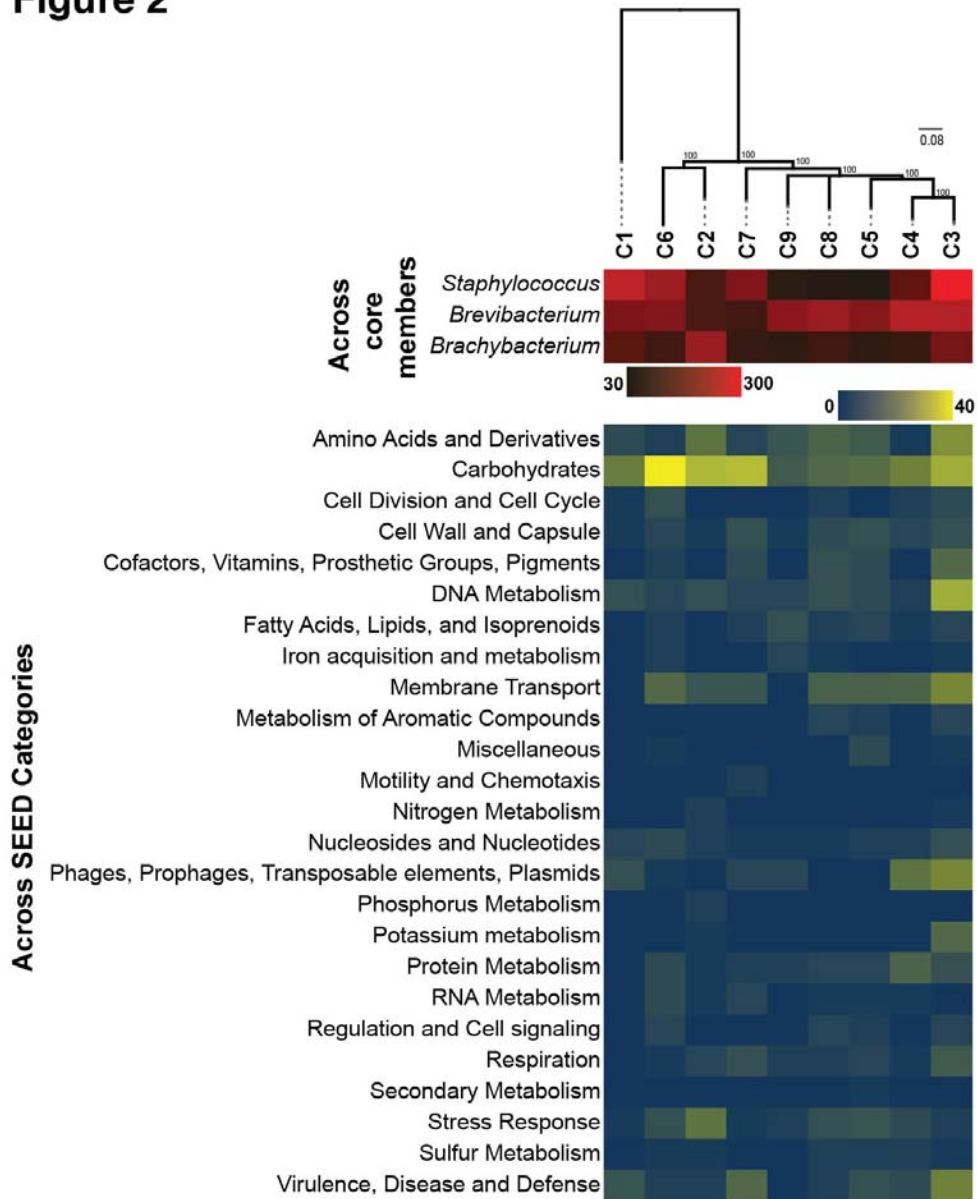
716 **Figure 1: Isolation of nine taxonomically identical cheese rind core microbiomes. (A)** The  
717 same three bacterial species - *Staphylococcus equorum*, *Brevibacterium auranticum*, and  
718 *Brachybacterium alimentarium* - were isolated from a set of 137 cheese rinds that were  
719 previously described using 16S rRNA gene amplicon sequencing (Wolfe et al. 2014). Each  
720 column represents average relative abundance data for one cheese rind microbiome. Data are  
721 clustered using an UPGMA tree based on Bray-Curtis dissimilarity. **(B)** The three core  
722 microbiome species have distinct colony morphologies. **(C)** Graphical representation of the nine  
723 core microbiomes as used throughout the manuscript.

724



725

**Figure 2**



726

727

728

729

730

731

732

733

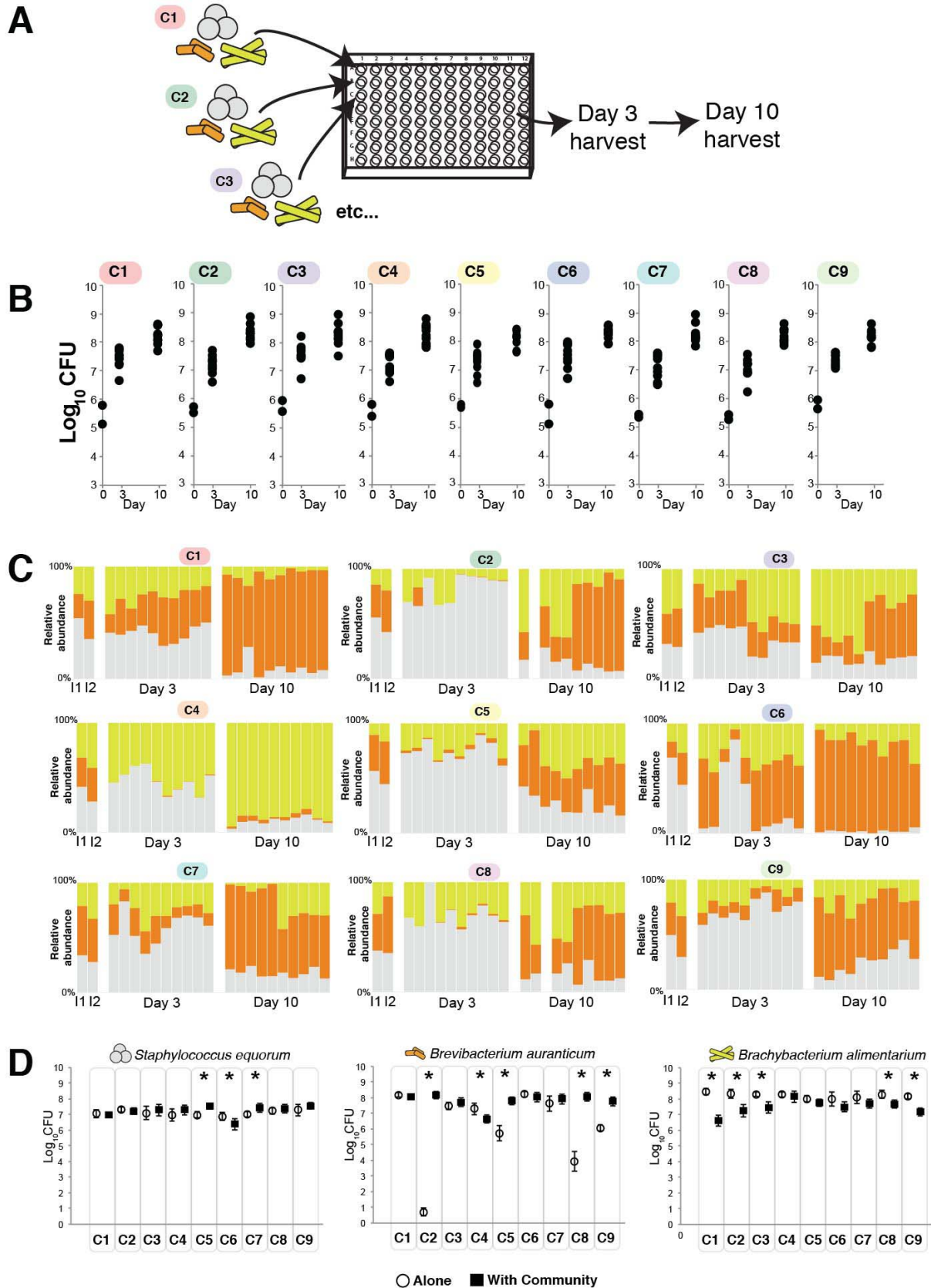
734

735

736

**Figure 2: Accessory genome of the cheese rind core microbiomes.** Heatmap indicates variation in the abundance of unique accessory gene clusters across the three individual taxa (top) and across SEED functional categories (bottom). Phylogeny is a maximum likelihood consensus tree constructed from SNPs identified across the nine core communities. Values are bootstrap support.

## Figure 3



738 **Figure 3 (previous page): Divergent community assembly across the nine cheese rind**  
739 **core microbiomes. (A)** Experimental setup. Each set of three species from each core  
740 microbiome was inoculated into wells of 96-well plates. Communities were harvested three and  
741 ten days after inoculation. **(B)** Total community abundance as measured by CFUs of each of the  
742 nine core microbiomes. n=5 across two experimental replicates. **(C)** Relative abundance of  
743 each of the three bacterial species across each of the nine core microbiomes. Each column  
744 represents a replicate. I1 and I2 indicate the input compositions for the two independent  
745 experimental replicates. In the Day 3 and Day 10 datasets, the first five columns are from one  
746 experimental replicate and the second five are from a second experimental replicate. Blank  
747 columns represent replicates that were lost due to contamination. **(D)** Growth of each of the  
748 community members alone (open circles) and in the presence of the community (closed black  
749 squares). Each point represents the mean CFUs of the taxa and the error bars represent one  
750 standard deviation of the mean. Asterisks indicate significant differences between growth alone  
751 and growth in the community (n=5, t-test,  $p < 0.05$ ).

752  
753  
754  
755  
756  
757  
758  
759  
760  
761  
762  
763  
764  
765  
766  
767  
768  
769  
770  
771  
772  
773  
774  
775  
776  
777  
778

779 **Figure 4 (next page): Response of the nine cheese rind core microbiomes to abiotic and**  
780 **biotic perturbations. (A)** Responses of each taxa to abiotic (6% salt) and biotic (*Penicillium*)  
781 disturbance. Each point represents the mean CFUs of the taxa in that community at Day 10  
782 (n=5) and the error bars represent one standard deviation of the mean. Asterisks indicate  
783 significant difference in growth compared to control based on Kruskal-Wallis test ( $p < 0.05$ ). (B)  
784 Mean community composition in the three treatments. Asterisk indicates significant difference in  
785 community composition compared to control based on PERMANOVA. (C) Principal coordinates  
786 analysis of replicate communities in the three treatments. PCoA is based on Bray-Curtis  
787 dissimilarity of absolute abundances of each community member.

## Figure 4

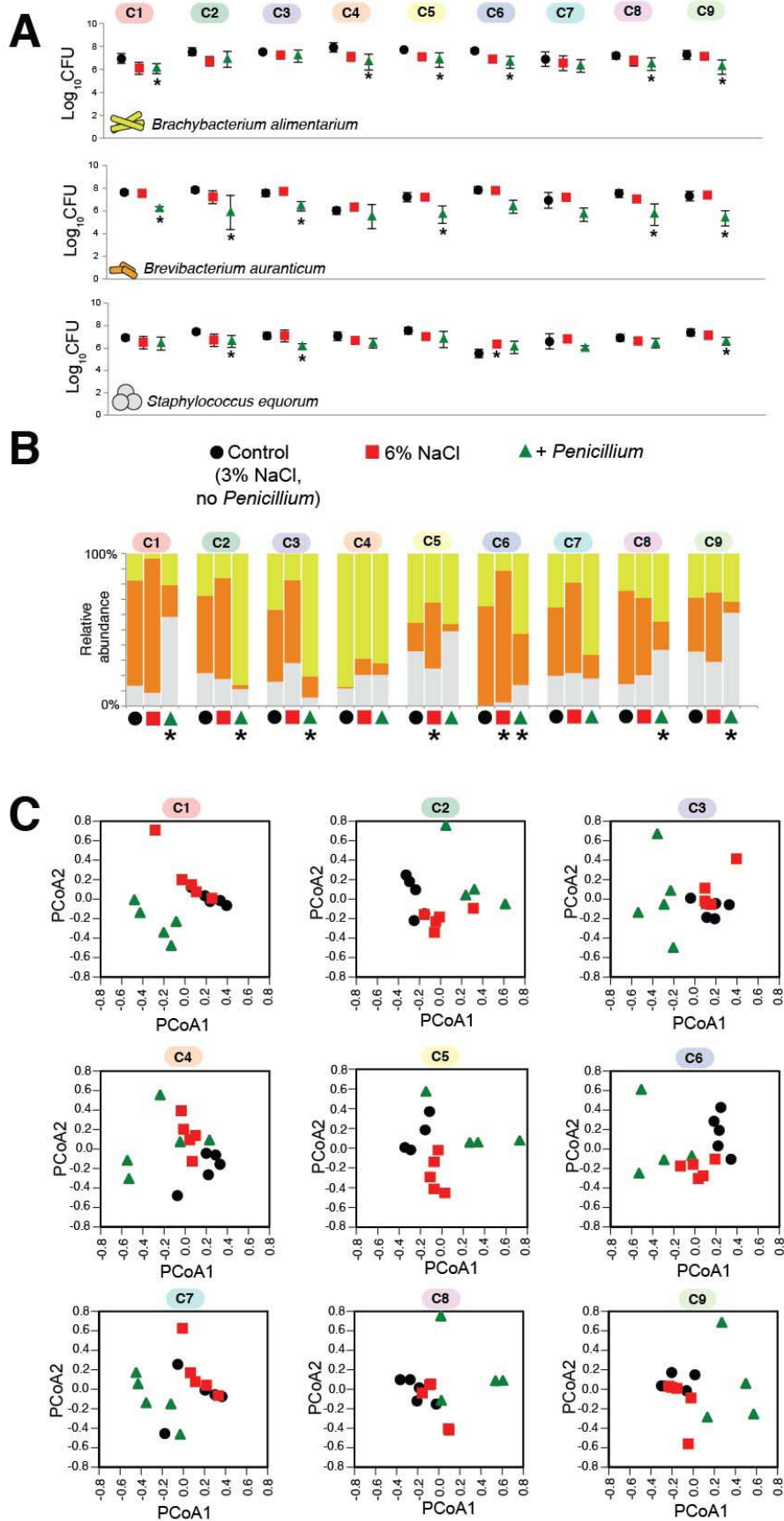
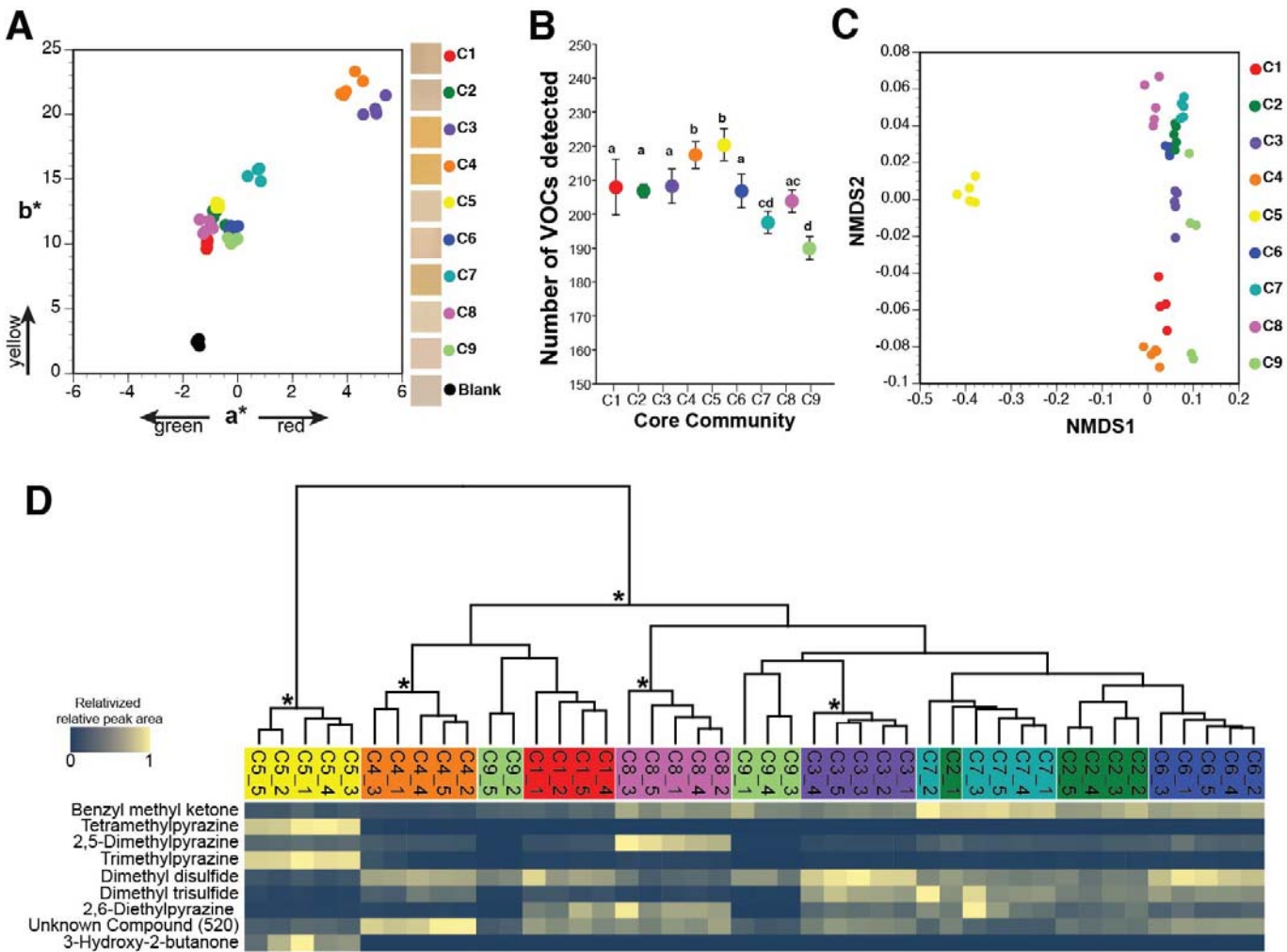


## Figure 5



789  
 790  
 791 **Figure 5: Functional diversity across nine cheese rind core microbiomes. (A)** Color  
 792 profiles of experimental rind communities after ten days of rind development. Each dot  
 793 represents a replicate cheese rind community (n=5). Boxes in legend are representative photos  
 794 of the experimental cheese surface from each community. **(B)** Total volatile organic compound  
 795 (VOC) diversity across the nine cheese communities. Each point represents the mean number  
 796 of VOCs detected in each community and the error bars represent one standard deviation of the  
 797 mean (n=5). Core communities that share the same letter are not significantly different from one  
 798 another based on Kruskal-Wallis test ( $p < 0.05$ ). **(C)** Non-metric multidimensional scaling of total  
 799 VOC profiles. Each dot represents a replicate cheese rind community (n=5). **(D)** Relative  
 800 abundance of VOCs that contributed the most to the Bray-Curtis dissimilarity across  
 801 communities (as determined by SIMPER analysis). Because total concentrations of VOCs are  
 802 highly variable across different compounds, visualization was simplified by relativizing the  
 803 relative peak area from GC-MS chromatograms within each VOC to the highest concentration  
 804 detected for that VOC. Data are clustered together by total VOC profiles using a UPGMA tree.  
 805 Asterisks indicate clusters with > 70% bootstrap support.

806 **SUPPLEMENTARY TABLES:**

807

808 **Table S1:** Overview of bacterial strains and genomes used in this study

809

810 **Table S2:** Distribution of gene clusters in the three taxa from each of the nine core  
811 microbiomes. When a cell is filled, it indicates that a predicted gene belongs to a gene  
812 cluster (row). In some communities, multiple genes belong to a single gene cluster. The  
813 identifiers in the cells are the gene IDs of each of the genomes based on the RAST  
814 annotation of that genome.

815

816 **Table S3:** Enrichment of SEED subsystem categories in core microbiomes based on  
817 Fisher's exact test.

818

819 **Table S4:** Relative peak area of each volatile organic compound detected from the  
820 experimental cheese communities. The "\_1, \_2, etc." indicates replicates within each of  
821 the nine core communities.

822